IEEE Access
Multidisciplinary ⋮ Rapid Review ⋮ Open Access Journal

Received January 4, 2022, accepted January 12, 2022, date of publication February 9, 2022, date of current version February 28, 2022.

Digital Object Identifier 10.1109/ACCESS.2022.3150345

Masked Face Recognition With Mask Transfer and Self-Attention Under the COVID-19 Pandemic

MENG ZHANG[1,2], RUJIE LIU[2], DAISUKE DEGUCHI[1], (Member, IEEE), AND HIROSHI MURASE[1], (Life Fellow, IEEE)

[1]Graduate School of Informatics, Nagoya University, Nagoya, Aichi 464-8601, Japan
[2]Fujitsu Research and Development Center, Beijing 100022, China

Corresponding author: Meng Zhang (zhang.meng@f.mbox.nagoya-u.ac.jp)

ABSTRACT Face masks bring a new challenge to face recognition systems especially against the background of the COVID-19 pandemic. In this paper, a method used for mitigating the negative effects of mask defects on face recognition is proposed. Firstly, a low-cost, accurate method of masked face synthesis, i.e. mask transfer, is proposed for data augmentation. Secondly, an attention-aware masked face recognition (AMaskNet) is proposed to improve the performance of masked face recognition, which includes two modules: a feature extractor and a contribution estimator. Therein, the contribution estimator is employed to learn the contribution of the feature elements, thus achieving refined feature representation by simple matrix multiplications. Meanwhile, the end-to-end training strategy is utilized to optimize the entire model. Finally, a mask-aware similarity matching strategy (MS) is adopted to improve the performance in the inference stage. The experiments show that the proposed method consistently outperforms on three masked face recognition datasets: RMFRD, COX and Public-IvS. Meanwhile, a qualitative analysis experiments using CAM indicate that the contribution learned by AMaskNet is more conducive to masked face recognition.

INDEX TERMS Masked face recognition, mask transfer, face synthesis, attention mechanism.

I. INTRODUCTION

The COVID-19 pandemic has created a global disaster: the World Health Organization (WHO) and Centers for Disease Control and Prevention (CDC) have suggested everyone should wear a mask in a public setting especially when other social distancing measures are difficult to maintain [4]. Face recognition is non-contact, highly efficient, user friendly, and so forth, and has been widely applied in access control and security authentication in public places; however, masks bring a new challenge to existing commercial face recognition techniques. Face recognition becomes more difficult when a large part of the face is covered by a mask. Therefore, it is essential to study the effect of wearing face masks on the behavior of face recognition systems and design mitigation techniques to offset the inevitable performance loss.

Deep-learning-based approaches predominate in the task of face recognition due to the emergence of advanced convolutional neural networks and large-scale datasets [5], [6]. Despite the success of deep learning models under general face recognition scenarios, the deep features still demonstrate imperfect invariance to wearing a mask, where the whole face image can't be provided for description. Therefore, the use of face masks triggers a significant research challenge: firstly, it is necessary to collect a large-scale training dataset, which includes the different types of faces with masks. In order to collect such a large-scale training dataset, on the one hand, it is time consuming and incurs higher labour cost, on the other hand, maintaining the diversity of data in such datasets is a slow process. Therefore, a low-cost, convenient face data augmentation method is needed as a matter of urgency. Secondly, it is essential to mitigate the performance loss from the perspective of model design according to the characteristics of face masks.

Some methods of simulating a masked face [7]–[10] have been proposed for face data augmentation. MaskTheFace [9] used a Dlib-based [11] face landmark detector to identify facial tilt and six key features of the face necessary for applying a mask. MaskedFace-Net [7], defined a mask-to-face deformable model and applied homographic transformation to map mask pixels over the targeted facial areas. However, these methods only utilize affine transformation,

The associate editor coordinating the review of this manuscript and approving it for publication was Derek Abbott.

and the added mask often looks unnatural; furthermore, those methods ignore pose and illumination consistency thus leading to biased masked face augmentation. Recently, Generative Adversarial Network (GAN) has become a powerful technique used in data augmentation [12], however, on the one hand, GAN-based method suffers from mode collapse deeply, which usually manifests as that the images thus generated by generator tend to have high similarity amongst them, even though their corresponding latent vectors have been very different. On the other hand, GAN-based methods are generally slow and difficult to run online in recognition. On the contrary, our method can quickly collect various types of mask images and can be transferred to the face image in run-time for the mask-aware similarity matching strategy in the inference stage.

Numerous approaches have been proposed to tackle the problem regarding occlusion which is a common problem in computer vision [2], [13]. Wearing a mask is considered the most difficult facial occlusion challenge since it covers most of the face including the mouth and nose. Anwar *et al.* [9] developed an open-source tool (MaskTheFace), to create a large dataset of masked faces, and then re-train existing face recognition systems to improve their accuracy. To reduce the negative influence of masks, in [14], the masked region is directly discarded when extracting deep features. Mundial, *et al.* [15] used a supervised learning approach and an in-depth neural network to recognize masked faces and extract individual facial features, with which an Support Vector Machine classifier was established for classification purposes.

The covered facial areas contain many salient features that make it useful for face recognition, such as the nasal region [16], but the extracted features of the covered facial areas are damaged due to occlusions caused by mask. Therefore, compared with uncovered facial areas such as the eye region, intuitively speaking, the mask area does not contain much discriminative information useful in recognizing a face, which gives us the hint that more attention should be paid to the uncovered region in feature extraction. Recently, attention mechanisms have been introduced to video face recognition systems [17], [18], where an attention mechanism is adopted to mimic human perception to focus on important information. Inspired by those works, an attention-aware masked face recognition model (AMaskNet) is proposed for masked face recognition, which lends more weight to useful features while (in relative terms) ignoring those corrupted by the face mask by learning a contribution matrix. Indeed, AMaskNet can localize the salient facial areas and extract more discriminative features from a non-masked face image and can alleviate the performance degradation of the non-masked scene. Even in low-quality face recognition scenes, the recognition performance of without wearing a mask is even slightly improved.

Herein, we qualitatively and quantitatively analyse the effect of wearing a mask on face recognition, and then propose a method for mitigating the negative effects of mask defects on face recognition. Firstly, a low-cost, accurate method of mask transfer is proposed for masked face synthesis by considering pose and illumination consistency. Secondly, an AMaskNet is designed to improve the performance of masked face recognition. The AMaskNet includes two modules,a feature extractor and a contribution estimator, wherein the latter is employed to learn the contribution of each spatial region which is then combined with the feature to improve its representation capability. An end-to-end training strategy is adopted to optimize the whole network. Finally, a mask-aware similarity matching strategy is proposed to improve the performance in the inference stage. The experiments show that the proposed method consistently outperforms on three masked face recognition datasets: RMFRD [1], COX [2] and Public-IvS [3]. Meanwhile, qualitative analysis experiments using CAM [19] indicate that the contribution learned by the AMaskNet is beneficial to masked face recognition. The main contributions are summarized thus:

(1) A low-cost, accurate mask transfer method for masked face data augmentation is proposed by the consideration of pose and illumination consistency. This method can add the mask from any face image with a mask to any face image without a mask.
(2) Qualitative and quantitative experiments are conducted to analyze the effect of wearing face masks on the behavior of face recognition systems.
(3) An AMaskNet is proposed to improve the performance of masked face recognition.
(4) A mask-aware similarity matching strategy is proposed for the inference stage, which can be applied to any face recognition scene in which one image with a mask and the other without a mask are present.

The paper is organized as follows: in Section 2 related work on masked face recognition is reviewed. Section 3 describes the proposed method of mask transfer, AMaskNet, and mask-aware similarity matching strategy. Section 4 presents the experimental results and the conclusion is given in Section 5.

II. RELATED WORK

A. METHODS OF SIMULATING MASKED FACE IMAGES

Recently, some methods of simulated masked face image have been proposed [7]–[10]. MaskTheFace [9] used a Dlib-based [11] face landmark detector to identify the face tilt and six key features of the face necessary for applying a mask. MaskedFace-Net [7] defined a mask-to-face deformable model and applied homographic transformation for mapping mask pixels over the targeted facial areas. Firstly, feature-based cascade classifiers are used to detect a region of interest in the facial image, with which a key-point detector is used to automatically detect 68 landmarks representing the facial structure. Besides, an image of a conventional face mask is selected as a reference image for the mapping where 12 key points are manually annotated for delineating the mask area. Finally, a homographic transformation is applied to

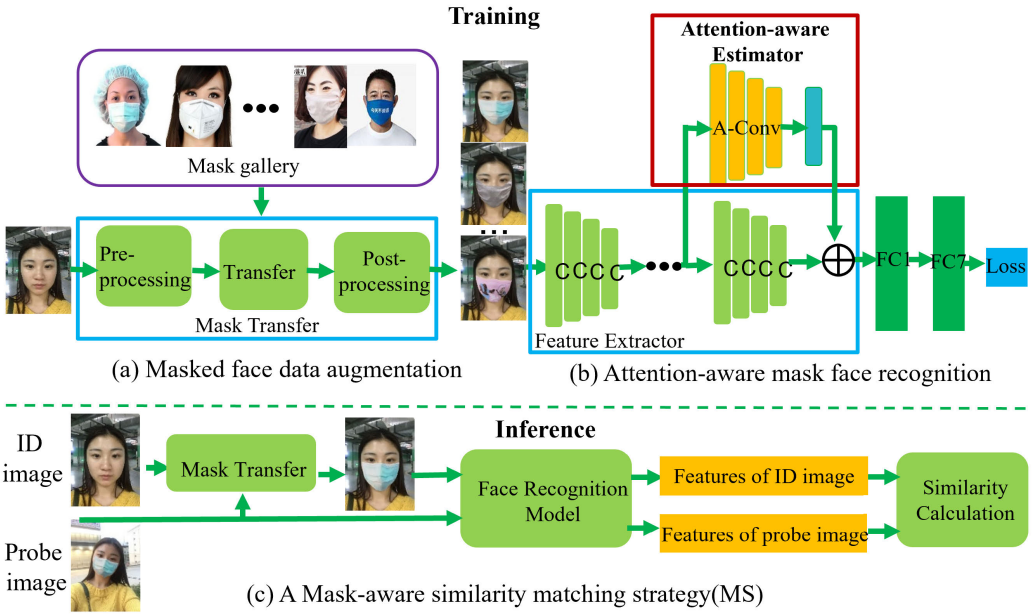

FIGURE 1. The architecture of our proposed method, which include the method of mask transfer, attention-aware mask face recognition (AMaskNet), and a mask-aware similarity matching strategy for inference. (Best viewed in color).

map mask pixels over the targeted facial areas relying on the defined point-to-point correspondence of landmarks between mask image and face image.

B. MASKED FACE RECOGNITION

Many different deep-learning-based approaches have been proposed to solve the occlusion problem. In 2014, Sun *et al.* [20] found that the features learned by DeepID2+ show certain robustness to image corruption in face verification tasks, and the combination of DeepID2+ features extracted from 25 face patches may further improve the robustness. Daniel *et al.* [13] used the augmented training data with synthetic occluded faces to tackle the occlusion problem. Recently, Masked face recognition has attracted much attention during the COVID-19 pandemic. Aqeel Anwar *et al.* [9] proposed an open-source tool, named MaskTheFace, to create masked face dataset from face dataset with extended feature support, and then used this dataset to re-train existing face recognition engines to improve their accuracy. Hariri and Walid [14] developed a reliable method based on occlusion removal and deep learning-based features to address the problem of the masked face recognition process. The first step is to remove the masked face region. Next, three pre-trained deep Convolutional Neural Networks (CNN) namely, VGG-16, AlexNet, and ResNet-50, are used to extract deep features from the obtained regions (mostly eyes and forehead regions). The Bag-of-Features paradigm is then applied to the feature maps of the last convolutional layer to quantize them and obtain a slight representation compared to the fully connected layer of classical CNN. Finally, a Multilayer Perceptron is applied for the classification process. Mundial *et al.* [15] used a supervised learning approach for masked face recognition together with in-depth neural network-based facial features. First, a CNN model was trained to generate an embedding of features of an image. Then they focused on a dataset which helps in building classifier for masked face, which consists of three images of a person, two masked face images, and one without a face mask. In the end, the Support Vector Machine is used for classification.

C. ATTENTION MECHANISMS IN FACE RECOGNITION

An attention mechanism is used to mimic human attention, which can concentrate on important information [21], [22]. Recently, attention mechanisms have been introduced to video face recognition [17], [18]. A meta attention-based aggregation scheme is employed in [18], to fine-grain the weights in an adaptive manner along each feature dimension among all frames to handle the features on a dimensional level. Rao *et al.* [17] used an attention-aware deep reinforcement learning method to discard misleading and confounding frames and find the focus of attention in video footage of faces.

III. PROPOSED APPROACH

In this section, the mask transfer method for masked face synthesis is firstly described by two stages: construction of a mask gallery and the generation of synthetic masked face images (Figs. 1(a) and 2). Secondly, the proposed AMaskNet is introduced. As shown in Fig.1(b), AMaskNet incorporates a feature extractor and a contribution estimator, and the contribution estimator further consists of two sub-modules, i.e., a self-spatial contribution estimator and a self-channel contribution estimator. The two sub-modules are used to learn

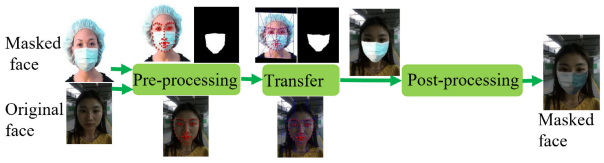

FIGURE 2. The flowchart of mask transfer. The masked face is a photo randomly selected from the mask gallery.

the spatial contribution and channel contribution respectively, and the refined features are obtained by combining the two contributions. Moreover, the entire network can be optimized through an end-to-end training procedure. Finally, a mask-aware similarity matching strategy is introduced for inference purposes, as illustrated in Fig. 1(c).

A. MASK TRANSFER (MT)

To generate the synthetic masked face image, a gallery of different masks should be firstly constructed. Given a non-masked face image and one mask from the gallery, the masked face image is obtained by transfer the mask, including pre-processing, transfer, and post-processing, as illustrated in Fig. 2.

1) COLLECTION OF MASK GALLERY

The construction of the mask gallery is aimed at obtaining a face image set covering versatile masks, such as different mask colors, shapes, and textures. For one mask type, only one face image with this mask is enough, therefore, it is easy to build this dataset through collection from website. Generally, any face image with a mask is qualified for the collection, however, to improve the quality of synthetic masked face images, the frontal view face images are preferable.

2) MASK TRANSFER FOR MASKED FACE SYNTHESIS

a: PRE-PROCESSING

Dlib [11] is used to detect 68 landmark points in both masked and non-masked face images. With these landmarks, a Triangulated Irregular Network is established and the facial area is thus divided into multiple triangular regions. Meanwhile, the grab-cut method [23] is employed to segment mask areas from masked face images.

b: TRANSFER

Transfer mask from masked face images to non-masked ones should be implemented based on the geometric relationship between the two faces. For each triangular piece in the Triangulated Irregular Network model, the affine transformation between the two images is calculated, and the mask region contained in this piece is transformed directly to a non-masked image. The whole mask will be transferred after all triangular pieces have been transformed.

c: POST-PROCESSING

Directly transferring the mask usually leads to inconsistency of illumination in the target image due to the lighting and contrast difference of the two images. For this problem, two post-processing steps are performed after the mask is transferred to the target image: (1) Alpha-matting is utilized to make the boundary more natural in terms of the transition across the boundary; (2) histogram specification is adopted to make the transferred mask region more illumination-consistent with the original non-masked face image. More specifically, the gray-scale distribution of the mask region is adjusted according to the gray-scale histogram of the original non-masked image, as shown in Fig. 7.

B. ATTENTION-AWARE NET FOR MASKED FACE RECOGNITION (AMaskNet)

The network architecture consists of two modules: a feature extractor and a contribution estimator, as illustrated in Fig. 3. A conventional face recognition scheme, e.g. ResNet34 [5], may be used for feature extraction, yielding a feature vector as the initial face representation. As mentioned previously, the face mask does not contain much subject-related information, so the extracted features are less discriminative. For this problem, the contribution estimator is designed to learn a contribution matrix to assign more weight to useful features while (in relative terms) ignoring those corrupted by the face mask. The contribution estimator as an attention scheme is implemented via a branch structure, which includes both spatial and channel components.

1) FEATURE EXTRACTOR

A conventional face recognition scheme (e.g., ResNet) can be used as a backbone for extraction of features, which is used as the baseline model. Recently, ArcFace [5] has achieved state-of-the-art performance and has been widely used in many papers. Here, we firstly adopt the ArcFace34 as our backbone, where BN-Conv-BN-PReLU-Conv-BN module as the residual bottleneck and all the convolution kernel size in residual bottlenecks have a size of 3×3. Then, the output feature of all models is fixed to 512-dimensions by a fully connected layer.

2) ATTENTION-AWARE CONTRIBUTION ESTIMATOR

The contribution estimator covers both spatial- and channel-wise measurements. They adaptively aggregate the feature maps in both channel and spatial domains to learn the inter-channel relationship and interspatial relationship matrices. The two matrices are then multiplied with the initial feature representation to produce refined face features. The sigmoid function is used instead of the ReLU [24] to map the output onto the interval [0,1], which is used as a contribution coefficient for weighting features. An end-to-end training strategy is adopted to optimize the entire network.

a: SPATIAL CONTRIBUTION ESTIMATOR

In order to estimate the contribution for each component of the feature map, a branch architecture is added to the backbone of the feature extractor model as the spatial contribution estimator, as shown in Fig. 3(b). In this process, a contribution

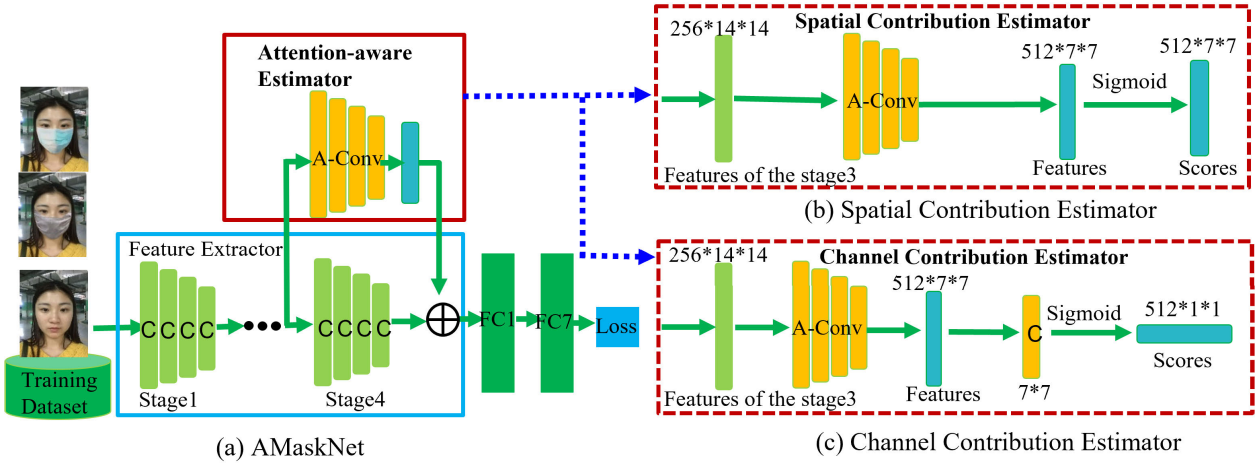

FIGURE 3. The architecture of AMaskNet. (b) Details of the spatial contribution estimator. (c) Details of the channel contribution estimator. The inputs of (a) and (b) are the outputs of a layer in the middle of the backbone network. The backbone is divided into four stages. Here we take the output of the third stage as an example. The network structure of A-Conv is the same as that of the Stage 4 of backbone of AMaskNet. The sigmoid function is utilized to map the output onto the interval [0,1], which is used as a contribution coefficient for weighting features. (Best viewed in color).

matrix is learnt which can assign greater weights to useful features while (in relative terms) ignoring those corrupted by the face mask. The contribution matrix and feature map have the same width and height. The structure of the spatial contribution estimator may have different complexities, ranging from one to several convolution layers. A more complex network may result in a better ability to learn, albeit at the cost of the extra computational effort and the risk of overfitting.

b: CHANNEL CONTRIBUTION ESTIMATOR

Akin to the spatial contribution estimator, a branch architecture is further added as the channel contribution estimator, in an attempt to estimate the contribution for each channel of the feature map, as shown in Fig. 3(c). In this module, a contribution matrix will be learnt to put more attention on useful channels. Similarly, different structures of various complexity may be adopted.

3) FEATURE AGGREGATOR

Let the feature extracted by feature extractor be $F_I \in R^{C*H*W}$, the spatial and channel contribution matrices be $C_S \in R^{C*H*W}$ and $C_C \in R^C$ respectively, the final feature is derived as:

$$F_C = C_C \otimes (C_S \oplus F_I) \tag{1}$$

where, $\otimes$ denotes matrix multiplication, $\oplus$ represents element-wise multiplication.

4) TRAINING STRATEGY

In model training, the ArcFace loss [5] is used to penalize identification errors. The bias is fixed as $b_j = 0$, logit is transformed as $W_j^T F_R = \left\| W_j^T \right\| \|F_R\| \cos\theta_j$, where θ_j is the angle between the weight W_j and the refined feature F_R. The individual weight is fixed as $\|W_j\| = 1$ by L_2 normalization. The refined feature is fixed as $| \|F_R\|$ by L_2 normalization and is re-scaled to s. This normalization makes the prediction probability only depend on the angle between the feature and the weight. So, the loss is formulated thus:

$$L_{id} = -\frac{1}{N}\sum_{i=1}^{N} \log \frac{e^{s(\cos(\theta_{y_i}+m))}}{e^{s(\cos(\theta_{y_i}+m))} + \sum_{j=1, j\neq y_i}^{N} e^{s(\cos\theta_j)}} \tag{2}$$

Here, m is the additive angular margin penalty between F_R and W_{y_i} to enhance the intra-class compactness and inter-class discrepancy simultaneously.

C. MASK-AWARE SIMILARITY MATCHING STRATEGY (MS)

In the real application, the two face photos for matching usually show different styles, that is, the ID or mug-shot photos coming from gallery are front portrait images without a mask, while the probe images captured on site sometimes are with a mask. Obtaining effective features by focusing more on the non-masked facial region is helpful in such situation, however, it still cannot eliminate the loss of accuracy caused by the presence of a mask. One straightforward method is to extract features only from upper facial regions when comparing two images with and without masks, but some important information will be neglected, e.g., shape information contained in the mask region. To solve this problem, a mask-aware similarity matching strategy (MS) is proposed, as illustrated in Fig. 1(c). This involves transfer of the mask from the masked face image to a non-masked image, thus mitigating the difference caused by the mask without loss of spatial information. This method can be applicable to any face recognition scene in which one image with a mask and the other without a mask is presented, especially useful for the 1:1 face verification scene.

IV. EXPERIMENT AND RESULTS

In this section, several benchmark datasets and several baseline models are firstly introduced. Then, some qualitative and quantitative analyses are undertaken to attain more insight into how the mask affects the performance of face recognition. Finally, the proposed mitigating models are compared with top-performing public models to confirm the effectiveness of our method.

A. DATASETS AND PROTOCOL

1) TRAINING DATASET

DeepGlint [25] is used as the training corpus. It includes cleaned MS-Celeb-1M [5] and the celebrity Asia dataset, achieving totally 6.6 million celebrity images of 172,000 celebrities therein. Due to the lack of a large volume of masked face photos to train the model, data augmentation is used for synthesizing masked face images by using the proposed mask-transfer technique. For each training image in DeepGlint, one mask image is randomly selected from the mask gallery and the mask is transferred to this training image. With this manner, the amount of training data is doubled, resulting in around 13M photos.

2) TESTING DATASET

Several commonly used benchmark datasets, such as RMFRD [1], COX [2], and Public-IvS [3], are used for testing.

COX [2] comprises 1,000 still images and 3,000 videos of 1,000 subjects. The video footage is captured using three cameras at different locations while the subjects are walking in a large gymnasium to simulate a surveillance scenario. The video-to-still (V2S) protocol proposed by the author is adopted for performance evaluation, where the true acceptance rate (TAR@FAR $= 10^{-4}$) is used for the 1:1 verification.

Public-IvS [3] designed for ID vs. spot face recognition, contains 1,262 identities and 5,503 images. The true acceptance rate (TAR @ FAR $= 10^{-5}$) for the 1:1 verification protocol is adopted to evaluate its performance.

To analyze the effectiveness of the proposed method on masked face recognition, the following four test conditions are designed to add masks to face photos given the test image pair in COX and Public-IvS, as shown in Fig. 4 and Fig. 5:

(1) Wo/Wo: no mask, original test images are used.
(2) W/W: different masks are added to both images in a pair to simulate a scene where both gallery and probe images are of masked faces.
(3) Wo/W: the recognition scene where gallery images do not contain masked faces, but probe images do. To simulate this condition, a mask is added to COX video frames (Public-IvS spot image) while keeping the COX still images (Public-IvS ID image) unchanged.

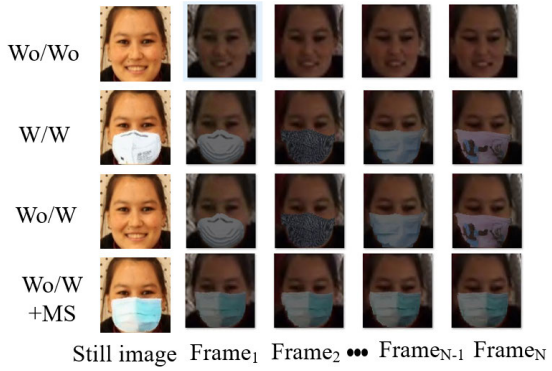

FIGURE 4. Some pairs of face image from the COX and COX-mask. Here, Wo/Wo: no mask, original test images are used. W/W: different masks are added to both images in a pair. Wo/W: the recognition scene where gallery images do not contain masked faces, but probe images do. Wo/W+MS: to improve the accuracy of Wo/W, the mask of the COX video frames is transferred to COX still images, i.e., the same masks are guaranteed to appear in each image pair.

FIGURE 5. Some pairs of face image from the Public-IvS and Public-IvS-mask (ID image vs. Spot image). Here, Wo/Wo: no mask, original test images are used. W/W: different masks are added to both images in a pair. Wo/W: the recognition scene where ID images do not contain masked faces, but spot images do. Wo/W+MS: to improve the accuracy of Wo/W, the mask of the spot image is transferred to ID images, i.e., the same masks are guaranteed to appear in each image pair.

FIGURE 6. Some pairs of face image from the RMFRD: face images without a mask (up) and with a mask (down).

(4) Wo/W+MS: to improve the accuracy of Wo/W, the mask of the COX video frames (Public-IvS spot image) is transferred to COX still images (Public-IvS ID image), i.e., the same masks are guaranteed to appear in each image pair.

RMFRD [1] is crawled from the Internet, including 5,000 pictures of 525 people wearing masks, and 90,000 images of the same 525 subjects without masks, which is mainly devoted to evaluate the existing face recognition system on masked images during the COVID-19 pandemic. Some sample images are illustrated in Fig. 6. The COX and private-IvS datasets are masked by the proposed mask transfer method, which is convenient to analyze the impact of masks on the performance of the model. However, to evaluate the performance of our model on the real-world masked face recogni-

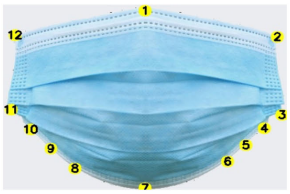

(a) Sample of mask gallery of MaskedFace-Net

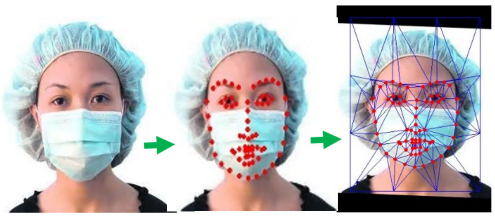

(b) Sample of mask gallery of our proposed method

(c) Results of MaskedFace-Net

(d) Results of our proposed method

FIGURE 7. Comparation of MaskedFace-Net [7] and our method. MaskedFace-Net requires manually labeling several key points on the mask boundary (a), while our proposed method automatically extracted the mask region from masked face image (b). Exemplar results when adding a mask are shown in (c) and (d) respectively.

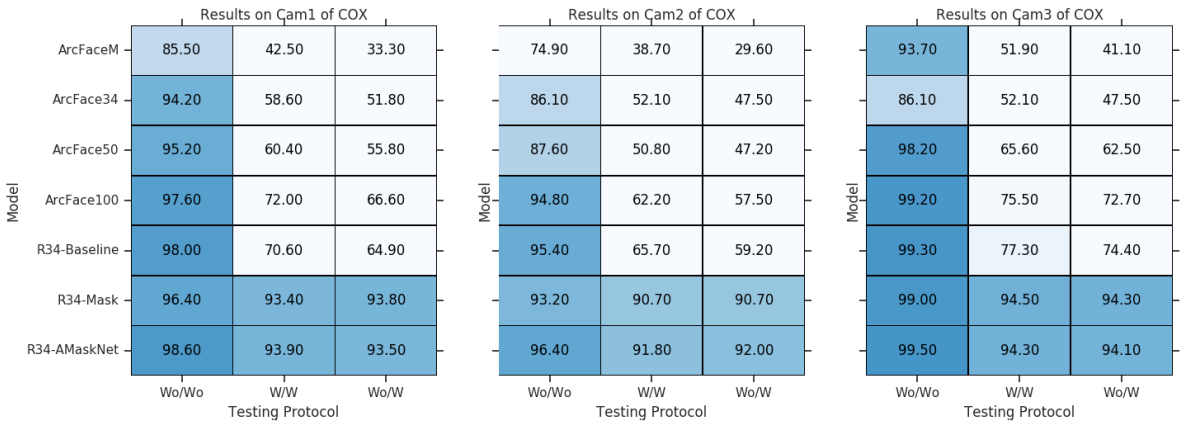

FIGURE 8. Results on COX dataset with 1:1 verification protocol at TAR@FAR = 10 − 4. Here, Wo/Wo: no mask, original test images are used. W/W: different masks are added to both images in a pair. Wo/W: the recognition scene where gallery images do not contain masked faces, but probe images do.

tion, experiments are conducted on the RMFRD dataset and compared with other state-of-the-art methods.

B. FACE RECOGNITION MODEL AND IMPLEMENTATION

1) FACE RECOGNITION MODEL

The ArcFace model [5], which has achieved state-of-the-art performance against several face recognition benchmarks such as LFW and YTF, is selected for comparisons. ArcFace introduces additive angular margin loss to enhance the discriminative power of the face recognition model, therefore, it is robust to the condition of wearing a mask. Four publicly available models, MobileFaceNet (ArcFaceM), LResNet34E-IR (ArcFace34), LResNet50E-IR (ArcFace50), and LResNet100E-IR (ArcFace100) are adopted. These models are downloaded from https://github.com/deepinsight/insightface/wiki/Model-Zoo. As introduced previously, the ResNet34 is selected in our method as the backbone for feature extraction, with which the DeepGlint without mask data augmentation is used to construct a baseline model to study the effect of face masks. To mitigate the negative effects of mask, two variants based on ResNet34 are established including data augmentation and the proposed attention scheme, as follows:

(1) R34-Baseline. A ResNet-34 model is trained with the original DeepGlint dataset, to quantify the loss of accuracy that the mask may induce.

(2) R34-Mask. A ResNet-34 model is trained by only the mask augmented DeepGlint dataset. This model can significantly improve the performance of masked-face recognition, but will degrade the performance of non-masked face recognition.

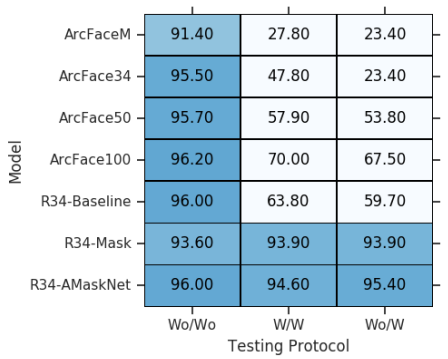

FIGURE 9. Results on Public-IvS dataset with 1:1 verification protocol at TAR@FAR = 10 − 5. Here, Wo/Wo: no mask, original test images are used. W/W: different masks are added to both images in a pair. Wo/W: the recognition scene where ID images do not contain masked faces, but spot images do.

(3) R34-AMaskNet. This is the proposed AMaskNet model trained with combination of the mask augmented DeepGlint and the original DeepGlint, which is expected to improve the performance of masked-face recognition while reducing the loss of accuracy inherent to non-masked face recognition.

2) IMPLEMENTATION

The ArcFace loss [5] is used to train the model, where the feature scale s is set to 64 and the *arccos* margin m is set to 0.5. In training, stochastic gradient descent is adopted with momentum and weight decay values of 0.9 and 0.0005, respectively. The training begins with a learning rate 0.1 for seven epochs, which is then decreased every five epochs by a factor of 10. A total of 25 epochs are taken for the training with the augmented DeepGlint dataset, and 760 images are used in each mini-batch.

C. EFFECTIVENESS OF THE PROPOSED METHOD

1) EFFECTIVENESS OF THE PROPOSED MASK TRANSFER FOR MASKED FACE SYNTHESIS

Fig. 7 illustrates some mask transfer examples. Figs 7(a) and 7(b) show the mask gallery of the traditional method and proposed method. The proposed method is simply a face image with a mask, which is easy to obtain and does not need manual annotation. It is low-cost, rapid, and convenient for model development. Figs 7(c) and 7(d) compare respectively the synthesized mask face images of the traditional method and the proposed method. From the results, it can be observed that the proposed mask transfer method is effective and can maintain consistency of illumination.

2) EFFECTIVENESS OF THE PROPOSED AMaskNet

a: RESULTS ON COX

As shown in Fig. 8, by re-training the R34-Baseline using a masked augmented dataset, the R34-Mask model achieves a significant improvement on images containing mask, e.g. a 28.9 percentage point improvement in Wo/W on Cam1 of COX; however, this method is likely to cause performance degradation in terms of general face recognition, e.g. a 1.6 percentage point decline in the case of Wo/Wo for the Cam1 of COX. The comparison between R34-AMaskNet and R34-Mask shows that AMaskNet is able to improve the performance, especially for masked face recognition, e.g. a 1.1 percentage point improvement in the case of W/W on the Cam2 of COX, which indicates that the proposed contribution estimator can learn an effective contribution matrix and automatically assign higher weights to the feature map activated by the non-masked facial parts and lower weights to those that are activated by masked facial parts. Meanwhile, the performance of R34-AMaskNet undergoes no significant decline and may even be slightly improved in the case of Wo/Wo. This is because COX is a low-quality video face recognition dataset with dramatic illumination and motion blur. However, AMaskNet can localize the salient facial areas and put more weight to discriminative features, thus improving the performance of wearing masks while minimizing the effect of general face recognition on existing face recognition systems.

b: RESULTS ON PUBLIC-IvS

As shown in Fig. 9, from the results on Public-IvS, a similar conclusion to the COX is obtained. Although R34-Mask can improve the performance of masks in the case of Wo/W or W/W, it will degrade the performance in the case of Wo/Wo. On the contrary, the R34-AMaskNet improves masked face recognition performance with a slight cost in terms of performance decrease in general face recognition.

3) EFFECTIVENESS OF THE PROPOSED MASK-AWARE SIMILARITY MATCHING STRATEGY (MS)

a: RESULTS ON COX

Table 1 shows the recognition result of without and with mask transfer on the Wo/W conditions (Wo/W vs. Wo/W+MS), where one contains a mask, while the other does not. In addition to R34-Mask and R34-AMaskNet models, the performance of the models is greatly improved after using the proposed mask-aware similarity matching strategy, e.g., an 11.3 percentage point improvement for ArcFaceM on the Cam2 of COX between images treated without mask-transfer to those with mask-transfer (because there is no mask strategy used therewith). Meanwhile, for R34-Mask and R34-AMaskNet, although the data augmentation strategy has been adopted, it is still improved in most cases, e.g., a 0.7 percentage point improvement for the R34-AMaskNet on the Cam2 of COX between images treated without mask-transfer to those with mask-transfer.

b: RESULTS ON Public-IvS

The comparison between without mask transfer (Wo/W) and with mask transfer (Wo/W+MS) on the Wo/W (one is with mask, while other is without mask) in Table 2 shows that the recognition performance is improved by using the mask-aware similarity matching strategy, especially for the general face recognition model, e.g. a 0.4 percentage point improvement for the R34-Mask, compared to a 14 percentage point

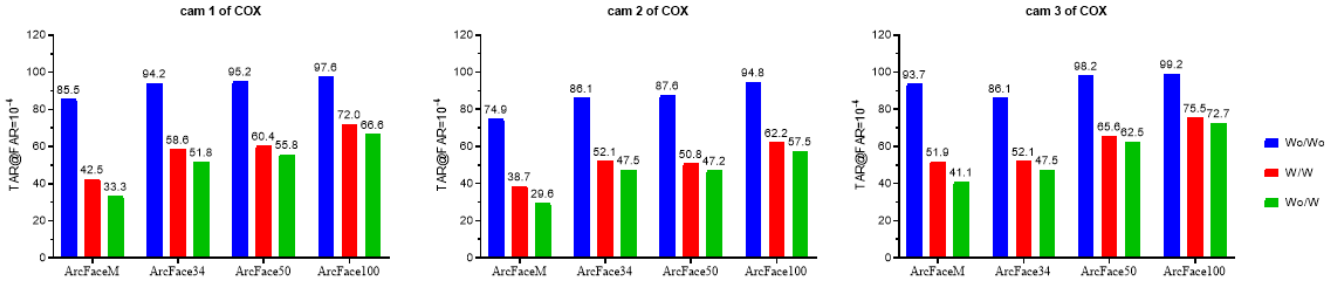

FIGURE 10. Results on COX dataset with a 1:1 verification protocol at TAR@FAR = 10 − 4. Here, Wo/Wo: no mask, original test images are used. W/W: different masks are added to both images in a pair. Wo/W: the recognition scene where gallery images do not contain masked faces, but probe images do.

TABLE 1. Results on COX dataset with 1:1 verification protocol at TAR@FAR=10^{-4}.

Model	Cam1		Cam2		Cam3	
	×	✓	×	✓	×	✓
ArcFaceM	33.3	41.4	29.6	40.9	41.1	55.8
ArcFace34	51.8	56.9	47.2	49.8	47.5	49.8
ArcFace50	55.8	59.8	47.5	50.7	62.5	68.2
ArcFace100	66.6	71.0	57.5	65.4	72.7	81.0
R34-Baseline	64.9	73.1	59.2	68.4	74.4	83.2
R34-Mask	93.8	92.9	90.7	92.2	94.3	98.6
R34-AMaskNet	93.5	93.0	92.0	92.7	94.1	98.5

✓means using the proposed mask-aware similarity matching strategy (Wo/W+MS), while × means not applicable (Wo/W).

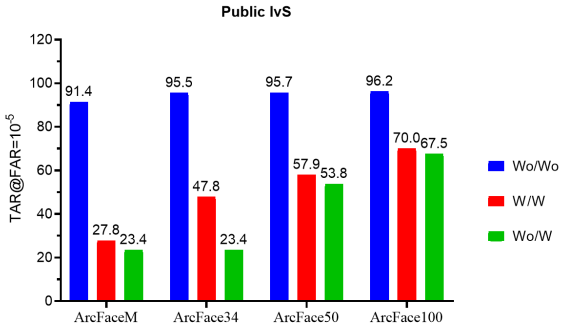

FIGURE 11. Results on Public-IvS dataset with 1:1 verification protocol at TAR@FAR = 10 − 5. Here, Wo/Wo: no mask, original test images are used. W/W: different masks are added to both images in a pair. Wo/W: the recognition scene where ID images do not contain masked faces, but spot images do.

TABLE 2. Results on public-IvS dataset with 1:1 verification protocol at TAR@FAR=10^{-5}.

Model	Public-IvS	
	×	✓
ArcFaceM	23.4	60.3
ArcFace34	23.4	60.3
ArcFace50	53.8	65.3
ArcFace100	67.5	75.7
R34-Baseline	59.7	70.8
R34-Mask	93.9	94.3
R34-AMaskNet	95.4	95.2

✓means using the proposed mask-aware similarity matching strategy (Wo/W+MS), while × means not applicable (Wo/W).

improvement for ArcFaceM on the Public-IvS dataset from without mask transfer to with mask transfer. The result shows that transfer the mask from masked image to non-masked

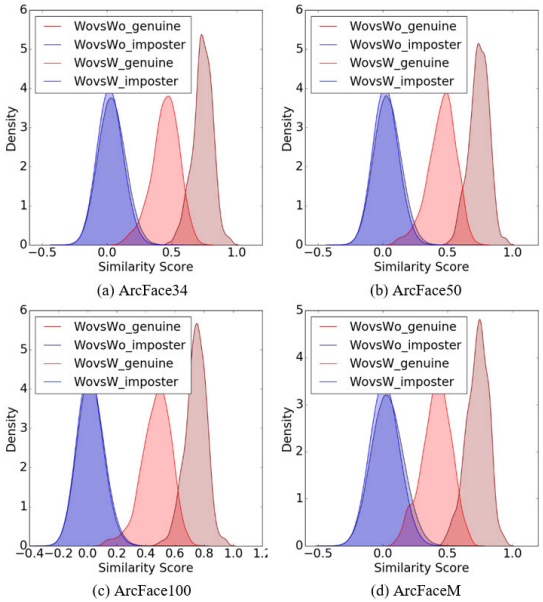

FIGURE 12. Distribution comparison of similarity scores on public model. Here, Wo denotes without wearing a mask, W means with wearing a mask.

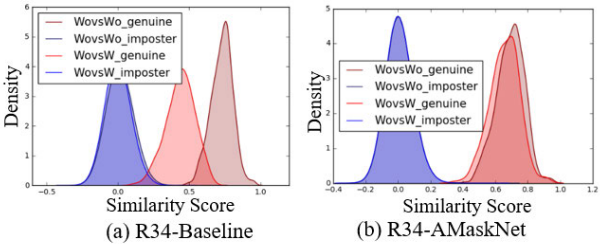

FIGURE 13. Distribution comparison of similarity scores. (a) In baseline model, the genuine scores significantly shift towards the imposter scores when the image is with a mask. (b) In R34-AMaskNet, the shift of similarity scores is largely mitigated. Here, Wo means without wearing a mask, W means with wearing a mask.

image in the face pairs can mitigate the difference caused by the mask without loss of spatial information in the inference stage.

D. COMPARISON OF STATE-OF-THE-ART METHODS ON RWMFD DATASET

The further to verify the effectiveness of the proposed method on real mask data, we compare our method, public models

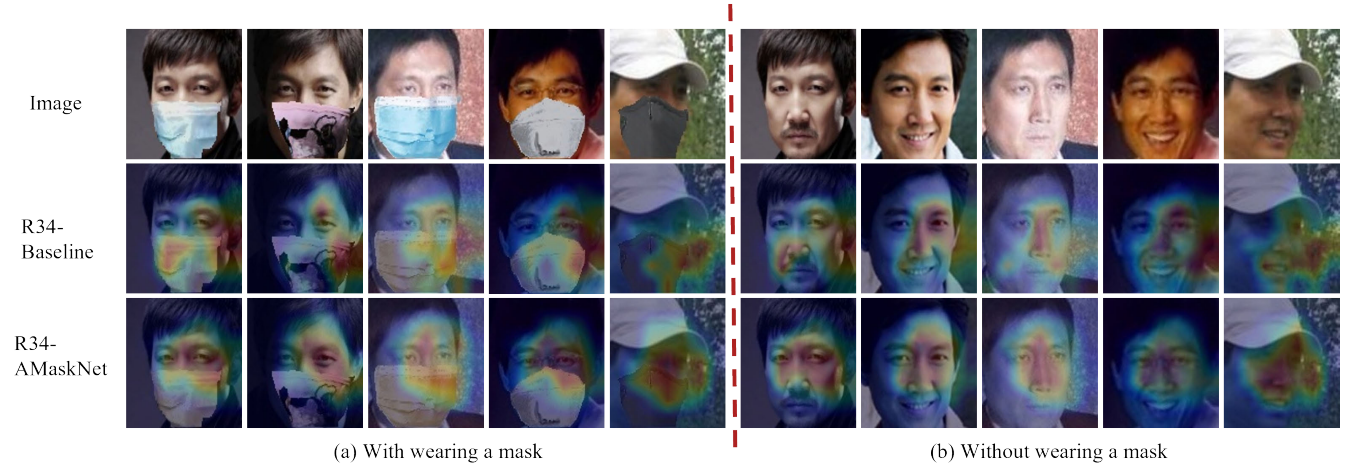

FIGURE 14. Visualization of attention result. (a) are the images with wearing a mask and its visualization results on R34-Baseline and R34-AMaskNet respectively. (b) are the images without wearing a mask and its visualization results on R34-Baseline and R34-AMaskNet respectively. From the first line to the third line are the original image, the attention results of R34-Baseline and R34-AMaskNet respectively. The maps highlight the discriminative image regions used for face recognition. The model with contribution module can be successfully able to localize the discriminative regions for face recognition.

and other literature models on RMFRD dataset, with the result shown in Table 3, where the results of literature methods are taken from the corresponding papers. The R34-AMaskNet outperforms R34-Baseline with an improvement of up to 12.5 percentage point. Meanwhile, R34-AMaskNet outperforms the competitive methods by a significant margin, which indicates the proposed method is efficient when applied to a real masked face recognition scenario.

E. EFFECT OF MASK ON PERFORMANCE

The four publicly available models are evaluated under three test conditions, i.e., Wo/Wo, W/W, and Wo/W, to study the effect of wearing a mask on recognition accuracy.

1) EFFECT ON COX

As shown in Fig.10, compared to the scene without a mask, the recognition accuracy is largely decreased when a mask is present. For example, on Cam1 of COX data, ArcFace50 decreases from 95.2% on Wo/Wo to 55.8% on Wo/W, resulting in a 39.4 percentage point loss of accuracy. This magnitude of decrease in accuracy affects all camera scenes of COX dataset. Moreover, the poorer the model performance, the greater the loss of accuracy, e.g. 52.2% and 31% losses in ArcFaceM and ArcFace100, respectively, from Wo/Wo to Wo/W. It is noteworthy that having one image with a mask while the other image without a mask has a greater adverse effect on performance than both having masks, e.g. the loss of accuracy of ArcFaceM from Wo/Wo to Wo/W is 52.2 percentage point, but only 40 percentage point from Wo/Wo to W/W.

2) EFFECT ON PUBLIC-IvS

The recognition results on Public-IvS are shown in Fig.11. Again, we obtain similar findings to CoX, that is, the recognition accuracy is largely decreased when a mask is present. For example, ArcFace50 decreases from 95.7% on Wo/Wo to 53.8% on Wo/W, resulting in a 41.9 percentage point loss of accuracy.

TABLE 3. Results on RWMFD dataset.

Method	Accuracy
J. Luttrel et al. [26]	85.7
Hariri et al. [27]	84.6
Almabdy et al. [9]	87.0
Walid Hariri. [14]	91.3
ArcFaceM	34.6
ArcFace34	43.2
ArcFace50	49.3
ArcFace100	61.7
R34-Baseline	81.9
R34-Mask	92.5
R34-AMaskNet	**94.3**

3) EFFECT OF THE SIMILARITY DISTRIBUTIONS

To understand the reason behind, we analyze the similarity score distributions of genuine and imposter pairs in Wo/Wo and Wo/W test conditions, with the result on Public-IvS dataset as shown in Fig. 12. The choice of FAR determines the score threshold, and then affects the results of TAR. In comparison with the Wo/Wo condition, the scores of genuine pairs strongly transfer towards the imposters when one image is with a mask (Wo/Wo vs. Wo/W). That means, the scores of genuine pairs become smaller and are nearer to imposter pairs due to the influence of masks, which will cause the TAR to become smaller at the same FAR, making them less recognizable leading to performance degradation.

F. QUALITATIVE ANALYSIS

1) THE DISTRIBUTIONS OF SIMILARITY SCORE

The matching score distributions of genuine and imposter pairs in Wo/Wo and Wo/W test conditions are presented

in Fig. 13. In comparison with the Wo/Wo condition, the scores of genuine pairs of the baseline model shift towards the imposter counterparts when one image is of a masked face (Wo/Wo vs. Wo/W), implying that the scores of genuine pairs decrease and are closer to those of imposter pairs due to the influence of masks, which makes them less recognizable. With the R34-AMaskNet system, however, the score distribution of the genuine pairs shifts only slightly toward imposter ones, which clearly confirms that a stronger recognition capability is obtained in R34-AMaskNet.

2) CONTRIBUTION ESTIMATION

We randomly select some samples from the testing dataset for visual analysis. Fig. 14 qualitatively shows the contribution estimation result using CAM [4] for the purpose of intuitive understanding. It is found from this result that R34-AMaskNet can focus on the non-masked regions and exclude the background for most samples, suggesting that discriminative regions for face recognition are obtained. Even in images without a mask, this attention scheme can also localize the facial area and eliminate background interference, this is why the model performs slightly better under Wo/Wo conditions.

V. CONCLUSION

An effective method is proposed with which to mitigate the effect of mask defects in face recognition. Firstly, a low-cost, accurate method of masked face synthesis is proposed for use in data augmentation and a mask-aware similarity matching strategy is developed, which is low-cost, rapid, and convenient for model development. Secondly, AMaskNet is developed to improve the performance of masked face recognition, which includes two modules: a feature extractor and a contribution estimator, and the latter is adopted to learn the contribution matrix, thus outputting refined features by successive matrix multiplication. This method can learn an effective contribution matrix and automatically assign higher weights to the feature map activated by the non-masked facial parts and lower weights to those that are activated by masked facial parts. Finally, a mask-aware similarity method is proposed for use in the inference stage to mitigate the difference caused by the mask without loss of spatial information. Both qualitative and quantitative analysis results show that the proposed model can mitigate the effects of mask defects in face recognition.

While the method is designed for masked face recognition, it can also be applied in other computer vision tasks, especially for other face-related applications such as facial attribute recognition.

REFERENCES

[1] Z. Wang, G. Wang, B. Huang, Z. Xiong, Q. Hong, H. Wu, P. Yi, K. Jiang, N. Wang, Y. Pei, H. Chen, Y. Miao, Z. Huang, and J. Liang, "Masked face recognition dataset and application," *CoRR*, vol. abs/2003.09093, pp. 1–3, Mar. 2020.

[2] Z. Huang, S. Shan, R. Wang, H. Zhang, S. Lao, A. Kuerban, and X. Chen, "A benchmark and comparative study of video-based face recognition on COX face database," *IEEE Trans. Image Process.*, vol. 24, no. 12, pp. 5967–5981, Dec. 2015, doi: 10.1109/TIP.2015.2493448.

[3] X. Zhu, H. Liu, Z. Lei, H. Shi, F. Yang, D. Yi, G. Qi, and S. Z. Li, "Large-scale bisample learning on ID versus spot face recognition," *Int. J. Comput. Vis.*, vol. 127, nos. 6–7, pp. 684–700, Jun. 2019, doi: 10.1007/s11263-019-01162-8.

[4] Vaccinated W Y B F, "How to protect yourself and others," *Centers Disease Control Prevention*, 2021.

[5] J. Deng, J. Guo, N. Xue, and S. Zafeiriou, "ArcFace: Additive angular margin loss for deep face recognition," in *Proc. IEEE/CVF Conf. Comput. Vis. Pattern Recognit. (CVPR)*. Long Beach, CA, USA: Computer Vision Foundation, Jun. 2019, pp. 4690–4699. [Online]. Available: http://openaccess.thecvf.com/content_CVPR_2019/html/Deng_ArcFace_Additive_Angular_Margin_Loss_for_Deep_Face_Recognition_CVPR_2019_paper.html

[6] Y. Kim, W. Park, M.-C. Roh, and J. Shin, "GroupFace: Learning latent groups and constructing group-based representations for face recognition," in *Proc. IEEE/CVF Conf. Comput. Vis. Pattern Recognit. (CVPR)*, Seattle, WA, USA, Jun. 2020, pp. 5620–5629, doi: 10.1109/CVPR42600.2020.00566.

[7] A. Cabani, K. Hammoudi, H. Benhabiles, and M. Melkemi, "MaskedFace-Net—A dataset of correctly/incorrectly masked face images in the context of COVID-19," *CoRR*, vol. abs/2008.08016, pp. 1–5, Aug. 2020.

[8] D. M. Escrivá, V. G. Mendonça, and P. Joshi, *Learn OpenCV 4 by Building Projects: Build Real-World Computer Vision and Image Processing Applications With OpenCV and C++*. Birmingham, U.K.: Packt, 2018. [Online]. Available: https://github.com/spmallick/learnopencv/tree/master/FaceMaskOverlay

[9] A. Anwar and A. Raychowdhury, "Masked face recognition for secure authentication," *CoRR*, vol. abs/2008.11104, pp. 1–8, Aug. 2020.

[10] D. E. King, "Dlib-ml: A machine learning toolkit," *J. Mach. Learn. Res.*, vol. 10, pp. 1755–1758, 2009. [Online]. Available: https://github.com/render-examples/fastai-v3

[11] J. Howard and S. Gugger, "Fastai: A layered API for deep learning," *Information*, vol. 11, no. 2, p. 108, 2020. [Online]. Available: https://github.com/davisking/dlib

[12] Y. Shen, P. Luo, P. Luo, J. Yan, X. Wang, and X. Tang, "FaceID-GAN: Learning a symmetry three-player GAN for identity-preserving face synthesis," in *Proc. IEEE/CVF Conf. Comput. Vis. Pattern Recognit.* Salt Lake City, UT, USA: Computer Vision Foundation, Jun. 2018, pp. 821–830. [Online]. Available: http://openaccess.thecvf.com/content_cvpr_2018/html/Shen_FaceID-GAN_Learning_a_CVPR_2018_paper.html

[13] D. S. Trigueros, L. Meng, and M. Hartnett, "Enhancing convolutional neural networks for face recognition with occlusion maps and batch triplet loss," *Image Vis. Comput.*, vol. 79, pp. 99–108, Nov. 2018, doi: 10.1016/j.imavis.2018.09.011.

[14] W. Hariri, "Efficient masked face recognition method during the COVID-19 pandemic," *CoRR*, vol. abs/2105.03026, pp. 1–8, May 2021.

[15] I. Q. Mundial, M. S. U. Hassan, M. I. Tiwana, W. S. Qureshi, and E. Alanazi, "Towards facial recognition problem in COVID-19 pandemic," in *Proc. 4th Int. Conf. Electr., Telecommun. Comput. Eng. (ELTICOM)*, Sep. 2020, pp. 210–214.

[16] M. Emambakhsh and A. Evans, "Nasal patches and curves for expression-robust 3D face recognition," *IEEE Trans. Pattern Anal. Mach. Intell.*, vol. 39, no. 5, pp. 995–1007, May 2017, doi: 10.1109/TPAMI.2016.2565473.

[17] Y. Rao, J. Lu, and J. Zhou, "Attention-aware deep reinforcement learning for video face recognition," in *Proc. IEEE Int. Conf. Comput. Vis. (ICCV)*. Venice, Italy: IEEE Computer Society, Oct. 2017, pp. 3951–3960, doi: 10.1109/ICCV.2017.424.

[18] N. Sankaran, S. Tulyakov, S. Setlur, and V. Govindaraju, "Metadata-based feature aggregation network for face recognition," in *Proc. Int. Conf. Biometrics (ICB)*, Gold Coast, QLD, Australia, Feb. 2018, pp. 118–123, doi: 10.1109/ICB2018.2018.00028.

[19] B. Zhou, A. Khosla, A. Lapedriza, A. Oliva, and A. Torralba, "Learning deep features for discriminative localization," in *Proc. IEEE Conf. Comput. Vis. Pattern Recognit. (CVPR)*. Las Vegas, NV, USA: IEEE Computer Society, Jun. 2016, pp. 2921–2929, doi: 10.1109/CVPR.2016.319.

[20] Y. Sun, X. Wang, and X. Tang, "Deeply learned face representations are sparse, selective, and robust," in *Proc. IEEE Conf. Comput. Vis. Pattern Recognit. (CVPR)*. Boston, MA, USA: IEEE Computer Society, Jun. 2015, pp. 2892–2900, doi: 10.1109/CVPR.2015.7298907.
[21] S. Woo, J. Park, J. Lee, and I. S. Kweon, "CBAM: Convolutional block attention module," in *Proc. 15th Eur. Conf.*, in Lecture Notes in Computer Science, vol. 11211, V. Ferrari, M. Hebert, C. Sminchisescu, and Y. Weiss, Eds. Munich, Germany: Springer, Sep. 2018, pp. 3–19, doi: 10.1007/978-3-030-01234-2_1.
[22] H. Ling, J. Wu, L. Wu, J. Huang, J. Chen, and P. Li, "Self residual attention network for deep face recognition," *IEEE Access*, vol. 7, pp. 55159–55168, 2019, doi: 10.1109/ACCESS.2019.2913205.
[23] C. Rother, V. Kolmogorov, and A. Blake, "'GrabCut': Interactive foreground extraction using iterated graph cuts," *ACM Trans. Graph.*, vol. 23, no. 3, pp. 309–314, Aug. 2004, doi: 10.1145/1015706.1015720.
[24] A. Krizhevsky, I. Sutskever, and G. E. Hinton, "ImageNet classification with deep convolutional neural networks," in *Proc. 26th Annu. Conf. Neural Inf. Process. Syst.*, Lake Tahoe, NV, USA, P. L. Bartlett, F. C. N. Pereira, C. J. C. Burges, L. Bottou, and K. Q. Weinberger, Eds., 2012, pp. 1106–1114. [Online]. Available: https://proceedings.neurips.cc/paper/2012/hash/c399862d3b9d6b76c8436e924a68c45b-Abstract.html
[25] Trillionpairs. (2018). *Challenge 3: Face Feature Test/Trillion Pairs*. [Online]. Available: http://trillionpairs.deepglint.com/overview
[26] J. Luttrell, Z. Zhou, Y. Zhang, C. Zhang, P. Gong, B. Yang, and R. Li, "A deep transfer learning approach to fine-tuning facial recognition models," in *Proc. 13th IEEE Conf. Ind. Electron. Appl. (ICIEA)*, May 2018, pp. 2671–2676.
[27] W. Hariri, H. Tabia, N. Farah, A. Benouareth, and D. Declercq, "3D face recognition using covariance based descriptors," *Pattern Recognit. Lett.*, vol. 78, pp. 1–7, Jul. 2016, doi: 10.1016/j.patrec.2016.03.028.

MENG ZHANG received the M.Sc. degree from the Beijing University of Technology, China, in 2016. He is currently pursuing the Ph.D. degree in intelligent systems with the Graduate School of Informatics, Nagoya University, Japan. Since then, he has been working as a Researcher with Fujitsu Research and Development Center Company Ltd., Beijing, China. His research interests include image processing, pattern recognition, face recognition, and deep learning.

RUJIE LIU received the B.S., M.S., and Ph.D. degrees in electronic engineering from Beijing Jiaotong University, in 1995, 1998, and 2001, respectively. Since then, he has been working as a Researcher with Fujitsu Research and Development Center Company Ltd., Beijing, China. He has published more than 40 articles and tens of inventions. His research interests include AI, pattern recognition, and image processing.

DAISUKE DEGUCHI (Member, IEEE) received the B.Eng. and M.Eng. degrees in engineering and the Ph.D. degree in information science from Nagoya University, Japan, in 2001, 2003, and 2006, respectively. He became a Postdoctoral Fellow at Nagoya University, in 2006. From 2008 to 2012, he had been an Assistant Professor at the Graduate School of Information Science. From 2012 to 2019, he was an Associate Professor with Information Strategy Office. Since 2020, he has been an Associate Professor at the Graduate School of Informatics. He is working on the object detection, segmentation, recognition from videos, and their applications to ITS technologies, such as detection and recognition of traffic signs. He is a member of IEICE and IPS, Japan.

HIROSHI MURASE (Life Fellow, IEEE) received the B.Eng., M.Eng., and Ph.D. degrees in electrical engineering from Nagoya University, Japan. In 1980, he joined Nippon Telegraph and Telephone Corporation (NTT). From 1992 to 1993, he was a Visiting Research Scientist with Columbia University, New York. He has been a Professor with Nagoya University, since 2003. His research interests include computer vision, pattern recognition, and multimedia information processing. He is a fellow of the IPSJ and the IEICE. He was awarded the IEEE CVPR Best Paper Award in 1994, the IEEE ICRA Best Video Award in 1996, the IEICE Achievement Award in 2002, the IEEE Multimedia Paper Award in 2004, and the IEICE Distinguished Achievement and Contributions Award in 2018. He received the Medal with Purple Ribbon from the Government of Japan in 2012.